A Modified Higher Order Power Filter for Grid-Connected Renewable Energy Systems

Arash Anzalchi, *Student Member, IEEE,* Masood Moghaddami, *Student Member, IEEE,* Amir Moghaddasi, *Student Member, IEEE,* Maneli Malek Pour, *Student Member, IEEE* and Arif Sarwat, *Member, IEEE*

***Abstract*—In order to reduce the influence of the grid harmonic currents and voltages, harmonic compensation is regularly implemented for a grid-tied inverter. In this paper a new topology of higher order power filter for single-phase grid-tied voltage-source inverters (VSI), named $L(LCL)_2$, is introduced. The subscript is added to the name to avoid confusion with *LLCL* filter. In the proposed design the inverter side inductance is divided into three parts, and the grid side inductor is removed. Also an additional resonant branch at the double of switching frequency is added to the traditional *LLCL* filter to attenuate high frequency harmonics. The total inductance of this filter is less than *LLCL* filter with the amount of the grid side inductor. A comparative study and discussions on the subject of the traditional *LLCL* filter and the proposed $L(LCL)_2$ filter have been conducted and assessed through both experimental hardware implementation and Matlab/Simulink-based simulation on a 700 W, 120V / 60 Hz single-phase grid-tied inverter. Also, a straightforward engineering design benchmark is suggested to discover parameters of the proposed $L(LCL)_2$ filter. It is concluded that, compared with the *LLCL* filter, the $L(LCL)_2$ filter not only has less voltage drop and total inductor size, but also has better performance on reducing high order current harmonics.**

***Index Terms*—Grid-tied voltage-source inverter (VSI), *LCL*-filter; *LLCL* filter; $L(LCL)_2$ filter; current harmonics; switching-frequency, Power quality.**

I. Introduction

RENEWABLE energy sources and distributed generation (DG) resources are mostly connected to the power grid through a grid-connected inverter [1]. In order to limit the excessive current harmonics which are mostly produced by the sine pulse width modulation (PWM), a low-pass power filter is usually put in between a voltage-source inverter (VSI) and the grid [2]. The use of the PWM system necessitates an output filter to limit the grid-injected current harmonics, satisfying the standards of IEEE 1547.2-2008 and IEEE 519-2014. *L*-filters are typically used, but they have the drawbacks of slow dynamic response and big inductor value [3], [4]. In comparison to a first-order *L* filter, an *LCL* filter can satisfy the standards for grid interconnection with notably smaller size and cost, primarily for applications in several kilowatts [5]–[7].

For industrial uses, price of the components is a vital aspect of selecting the power filter of the grid-tied inverter. Owing to the growing cost of copper, various methods have been implemented to cut down the price of the power filter. One helpful way is to increase the switching frequency of the inverter where the method, surely, depends on the device proficiency and cost.

Nowadays, most power electronic designs are limited by thermal constraints. Power dissipation and surface area have a major influence on temperature increase. The volume and size of the component are two measures that the surface area of the object is directly linked with. The use the total power loss of the *LCL* filter as the optimization factor in the design was introduced in [8]. It explores the *LCL* filter design method from the perspective of efficiency and reduction in size and weight (and therefore cost) of the filter.

Special topologies or controls are other measures that have been focused on by researchers. In [9] a three-level neutral point clamped (NPC) converter as a high power renewable energy grid interface was introduced, trying to achieve higher switching frequency and efficiency. In [10], the LLCL-filter topology with two resonant circuits between the ripple inductor and the grid-side inductor to decrease the two dominant harmonic currents around the switching frequency and the double of switching frequency was proposed.

Moreover, LCL filter and LLCL filter colleagues have been studied in a number of different papers. For example, Ref. [11] examines the conducted Electromagnetic Interference (EMI) issues for the high-order power-filter-based single-phase full-bridge grid-tied inverter by means of the unipolar modulation in discontinuous mode. In order to minimize the additional reactive power as well as to achieve a small value of capacitor, a Differential Mode EMI suppressor for the LLCL-filter based system was proposed in [12]. To decrease the overall inductance value, without increasing the capacitive reactive power, modified LCL-filter topology using an extra parallel LC resonant circuit was suggested in [13]. A capacitor-current-feedback active damping by means of reduced computation delay was proposed in [14]. By using this method, the virtual impedance functions more similar to a resistor in a broader frequency range, and the unstable poles of the open loop are eliminated; consequently, great robustness against the grid-impedance deviation is attained. The magnetic integration of the LCL filter in grid-connected inverters was investigated in [15]. By placing the windings accurately and sharing an ungapped core, the major fluxes created by the two inductors of an LCL filter cancel out mostly in the common core.

As the further work of [16], this paper is to propose a modified high-order filter design, named $L(LCL)_2$ filter based on the *LLCL* filter. This filter can reduce the harmonics at the switching frequency and multiples of the switching frequency, while saving the total inductance and thereby leads to size

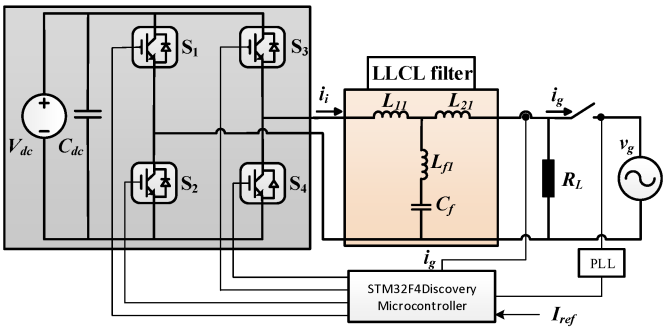

Fig. 1. Schematic diagram of the LLCL filter.

reduction of the filter. The most important role of the grid side inductor in the traditional *LLCL* filter is to decrease the harmonics around the twice of the switching frequency. In the new topology, this inductor is removed, and the converter side inverter of the filter is split into three parts. Then, two resonant traps at switching frequency and double of switching frequency are inserted in between the converter side inductor. The proposed filter is able to attenuate the current ripple components better than the *LCL* and traditional *LLCL* filters. This study can pave the path for the design and implementation of the *L(LCL)*$_2$ filter in VSI applications. This work has also presented the tools for further exploring the *L(LCL)*$_2$ filters for other case studies, such as analyzing stability of the system, optimizing the filter parameters, designing damping methods and EMI suppressor for the filter, etc.

The outline of the rest of the paper is as follows. First, the principle of an *LLCL* filter is presented for a single-phase power converter. Then, a new engineering design procedure of the high order power filter is proposed and the related analysis is done. Finally, experimental results on a 700 W, 120 V /60 Hz single-phase grid-tied inverter prototype with *LLCL* and *L(LCL)*$_2$ filters are carried out and compared to confirm the correctness of the theoretical analysis.

II. Principle Oof *LLCL*-Filters

The circuit configuration of an *LLCL*-filter-based single-phase grid-tied VSI is shown in Fig. 1. The inverter output voltage and current of the *LLCL* filter are represented as v_i and i_i, and the grid voltage and current are represented as v_g and i_g. The switching frequency is shown as f_s (in hertz) or ω_s (in radians per second).The power grid is assumed to be a perfect voltage source with zero impedance, to supply a continuous voltage at the frequency of 60 Hz.

The output voltage v_i(t) of the single-phase full-bridge voltage source inverter (VSI) can be calculated as (1), while it is utilized under the situation of sine-triangle, unipolar, and asymmetrical regular sampled PWM [17].

$$v_i(t) = mV_{dc}cos(\omega_0 t) + \sum_{k=1}^{\infty}\sum_{n=\pm1}^{\pm\infty} \frac{2V_{dc}J_n(k\pi m)}{k\pi}\sin(\frac{n\pi}{2})\cos(k\omega_s t + n\omega_0 t) \quad (1)$$

where m is the modulation index, V_{dc} is the dc link voltage, ω_0 is the fundamental frequency in radians per second, and $J_n(x)$ is referred as the integrals of the Bessel function, which is known as: $J_n(x) = \int_0^{\pi} cos(n\pi - xsint)dt$, representing the sideband harmonic magnitude.

The inverter output impedance while $\omega \neq \omega_0$ can be written as

$$Z_0(j\omega) = \frac{v_i(j\omega)}{i_i(j\omega)}|_{v_g(j\omega)=0} = \frac{(L_{11}L_{21}C_f + (L_{11}+L_{21})L_fC_f)(j\omega)^3 + (L_{11}+L_{21})(j\omega)}{(L_{21}+L_f)C_f(j\omega)^2 + 1} \quad (2)$$

Considering the harmonic current recommendation in 519-2014 and IEEE 1547.2-2008 [18], [19] the grid-side current i_g is supposed as the ideal continuous current at the fundamental frequency. With that in mind, the branch circuit of inductor L_{21} can be seen opened by considering the effects of the inverter high-frequency harmonics. Then (2) can be approximately rewritten as follows

$$Z_0(j\omega) = \frac{v_i(j\omega)}{i_i(j\omega)}|_{\omega\neq\omega_0} = L_{11}j\omega + L_{f1}j\omega + \frac{1}{C_fj\omega} \quad (3)$$

Additionally, $1/C_fj\omega \ll L_{11}j\omega$ is almost always true around the switching frequency or higher in an *LLCL* filter. Then, (3) can be simplified as

$$Z_0(j\omega) = \frac{v_i(j\omega)}{i_i(j\omega)}|_{\omega\neq\omega_0} = L_{11}j\omega + L_{f1}j\omega \quad (4)$$

And the amplitudes of harmonics of inverter-side current i_i can be derived as

$$|I_H||_{\omega\neq\omega_0} = \frac{|V_H(n,k)|}{|Z_0(j\omega)|} \quad (5)$$

where the amplitude output voltage harmonic $V_H(n,k)$ is

$$V_H(n,k) = |\frac{2V_{dc}J_n(k\pi m)}{k\pi}sin(\frac{n\pi}{2}) \quad (6)$$

when $k = 1, 2, ..., \infty$ and $n = \pm1, \pm2, ..., \infty$

Fig. 2 shows the main harmonic current power density spectrum of the inverter output current in the hardware setup, when the dc link voltage V_{dc} is 350 V, the modulation index m is 0.9, inverter-side current ripple is 24.1%I_{ref} (I_{ref} is fundamental peak current), and the switching frequency f_s is 20 kHz. As can be seen, the topmost harmonics of inverter output current are around the switching frequency and then the multiples of switching frequency. Consequently, the paralleled trap $L_{f1}C_f$ is mainly limited by the harmonics around the switching frequency and the grid-side inductor L_{21} is limited by double of switching frequency [20], [21].

Assuming that the grid is an ideal sinusoidal voltage source, the transfer functions $i_i(s)/v_i(s)$ be calculated as (7):

$$G_{u_i\rightarrow i_i}(s) = \frac{i_i(s)}{v_{i(s)}}|_{v_g(s)=0} = \frac{(L_2+L_f)C_fs^2+1}{(L_1L_2C_f + (L_1+L_2)L_fC_f)s^3 + (L_1+L_2)s} \quad (7)$$

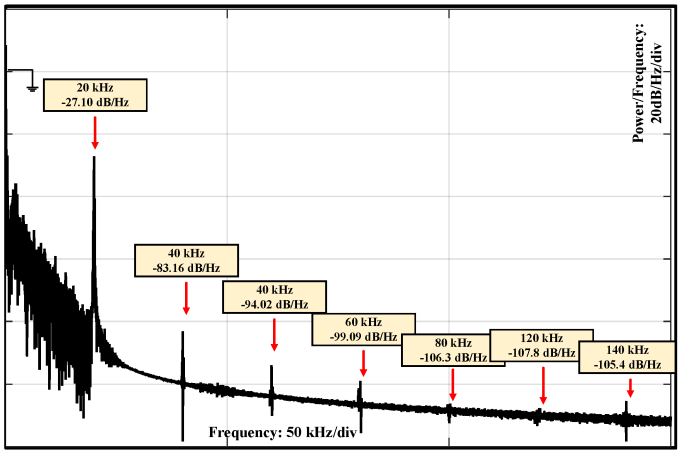

Fig. 2. Main harmonic current power density spectrum of inverter using unipolar modulation.

and the transfer functions $i_g(s)/v_i(s)$ of *LLCL* filter can be expressed as:

$$G_{u_i \to i_g}(s) = \frac{i_g(s)}{v_{i(s)}}|_{v_g(s)=0} = \frac{L_f C_f s^2 + 1}{(L_1 L_2 C_f + (L_1 + L_2) L_f C_f) s^3 + (L_1 + L_2) s} \quad (8)$$

III. PROPOSED *L(LCL)*$_2$ FILTER

In this paper, a new topology of the *LLCL* filter structure is proposed, as also illustrated in Fig. 3, where the inverter side inductance of the *LLCL* filter is separated into three sections to allow inserting resonant traps in between them. Also the resonant capacitor of the traditional *LLCL* filter is divided into two capacitors to produce a new resonant branch at double of switching frequency. Consequently, the grid side inductance of the *LLCL* filter (L_{21}) can be removed. As a result, since the total amount of the capacitor does not change, the capacitive reactive power at rated load will remain constant. Compared to the conventional *LLCL* filter-based system, not only does not the additional trap inserted between grid side inductance add to the control difficulties of the system, but also it reduce the size of the electromagnetic part of the system, which leads to a more efficient and cheaper low pass filter. Considering A(s) and M(s) definitions as below

$$A(s) = \frac{Z_2(s) Z_{f2}(s)}{Z_2(s) + Z_{f2}(S)}, M(s) = \frac{Z_2(s)}{Z_{f2}(s)} + 1 \quad (9)$$

Where $Z_1(s)=sL_{12}$, $Z_2(s)=sL_{22}=sL_{32}$, $Z_{f1}(s)=sL_{f1}+1/sC_{f1}$ and $Z_{f2}(s)=sL_{f2}+1/sC_{f2}$. And assuming grid is an ideal sinusoidal voltage source, the transfer functions $i_1(s)/v_i(s)$ and the transfer functions $i_g(s)/v_i(s)$ of *L(LCL)*$_2$ filter can be, respectively, derived as:

$$G_{u_i \to i_i}(s) = \frac{i_i(s)}{v_{i(s)}}|_{v_g(s)=0} = \frac{A + Z_2 + Z_{f1}}{(A + Z_2 + Z_1) Z_{f1} + (A + Z_2) Z_1} \quad (10)$$

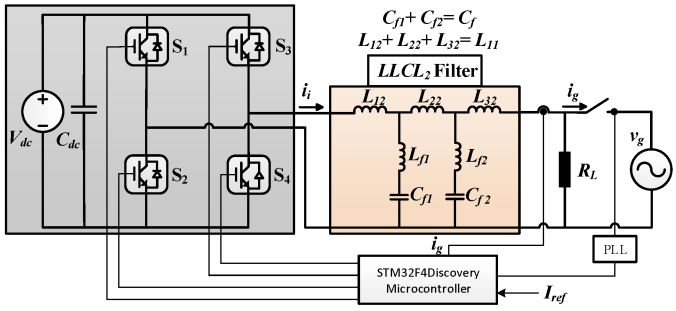

Fig. 3. Proposed *L(LCL)*$_2$ system.

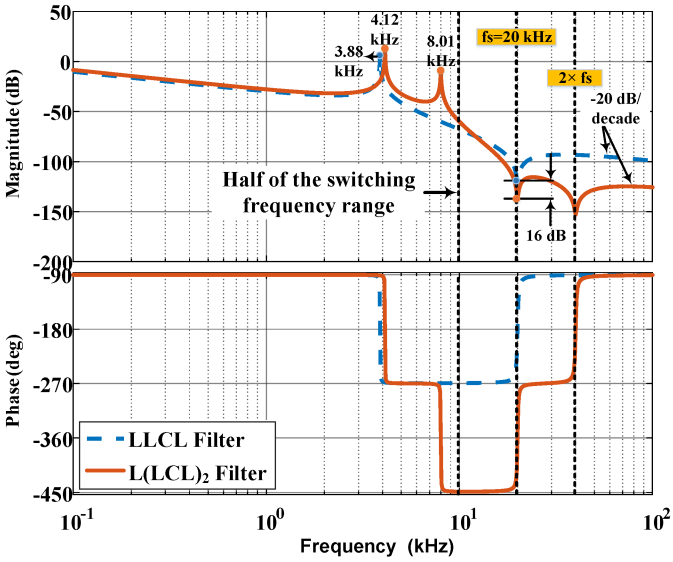

Fig. 4. Bode plots of transfer functions $i_g(s)/v_i(s)$.

$$G_{u_i \to i_g}(s) = \frac{i_g(s)}{v_{i(s)}}|_{v_g(s)=0} = \frac{Z_{f1}}{Z_2(M + Z_{f1}(M + Z_2) + 1) + M Z_1 Z_{f1}} \quad (11)$$

Fig. 4 shows the transfer function $i_g(s)$ / $v_i(s)$ of both the *L(LCL)*$_2$ filter and the *LLCL* filter while all the other parameters are the same except inductances of the traps. Also L_{11} in *LLCL* filter is divided into three parts and C_f is divided into two capacitors. Fig. 5 presents the transfer function $i_i(s)$ / v_i (s) with aforementioned parameters. The figures help in verifying that all the requirements are satisfied with the design. It can be recognized that within half of the switching frequency range, the *L(LCL)*$_2$ filter has almost the same frequency response pattern of an *LLCL* filter and both of resonant frequencies match the resonant frequency criteria of low pass filters for having a stable system. That is to say, compared with an ordinary *LLCL* filter, the additional $C_{f2}L_{f2}$ branch of the *LLCL* filter does not bring any further control worries.

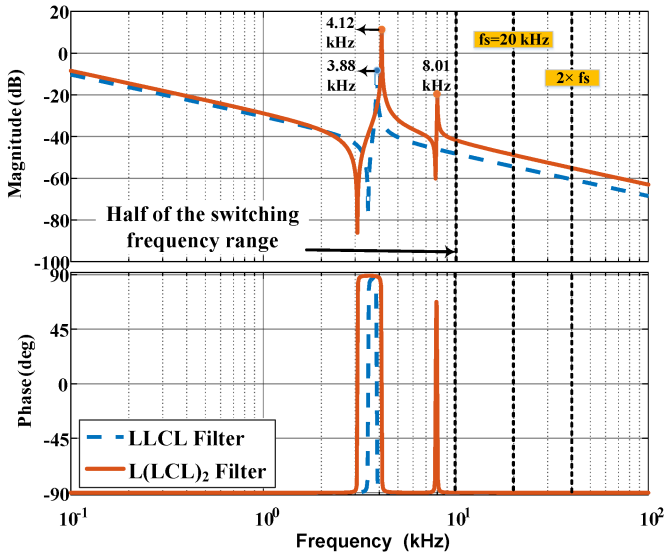

Fig. 5. Bode plots of transfer functions $i_i(s)/v_i(s)$.

A. Parameter Design of the L(LCL)$_2$ Filter

Some limitations were introduced by [4], [16], [22] to be considered when designing the power filters, an *LCL* and *LLCL* that could be used in *L(LCL)*$_2$ filter.

1) The total capacitive reactive power at rated load should be less than 5% of the nominal power and the capacitors are limited by this constraint.
2) The total inductance is limited by the voltage drop during operation (lower than 10%). Otherwise, the dc-link voltage will be required to be higher to assure current controllability, which will result in greater losses in switching devices.
3) The range of the resonant frequency ought to be between ten times the line frequency or one sixth of the switching frequency (whichever is bigger) [23] and one-half of the switching frequency, to keep away from stability and control problems may cause by resonance in the lower and upper parts of the harmonic spectrum.
4) The inverter-side inductor L_{12} is constrained by the requirement of the maximum ripple current (generally lower than 40%).
5) Considering IEEE 519-2014, the harmonics upper than the 35^{th} should be limited. For a grid-tied inverter system, each of the harmonic currents of greater than the 35^{th} have to be less than 0.3% of the rated fundamental current, if the short-circuit current of the system is less than 20 times the nominal grid-side fundamental current.

Considering mentioned constraints, the *L(LCL)*$_2$ filter can be designed by using the following step by step procedure.

1) With the intention of meeting a specific current ripple requirement, the inductance can be designed from the equation:

$$\frac{V_{dc}}{4f_s(\alpha_1 I_{ref})} \geq L_{11} \geq \frac{V_{dc}}{4f_s(\alpha_2 I_{ref})} \tag{12}$$

where, I_{ref} is the rated reference peak current, α_1 and α_2 are the inverter-side current ripple ratio, which generally have the value of 15% and 40% respectively. This inductance is the amount of total inductance of the filter (L_{11}=L_{21} +L_{22}+L_{23}) while L_{21} = K×L_{11} (33%<K<60%) and L_{22}=L_{23}=(L_{11} - L_{21})/2.
2) By selecting the absorbtion of reactive power while the system is operating in rated conditions, the capacitor value can be determined.

$$C_f(Total) = xC_b \tag{13}$$

where x is a percentage of the reactive power absorbed at rated conditions ($x < 1$). The total capacitor value is limited by the below condition

$$C_{max} = \frac{5\%P_{rated}}{{V_g}^2\omega_0} \tag{14}$$

Then the capacitor of each branch is almost half of the total capacitor.
3) As $L_{f1}C_{f1}$ and $L_{f2}C_{f2}$ circuit resonate at the switching frequency and the double of the switching frequency, then, L_{f1} and L_{f2} can be calculated as:

$$\frac{1}{\sqrt{L_{f1}C_{f1}}} = \omega_{s1}, \frac{1}{\sqrt{L_{f2}C_{f2}}} = \omega_{s2} \tag{15}$$

where, ω_{s1} is the switching frequency and ω_{s2} is twice the switching frequency in radians per second.
4) Grid side inductance L_{21}: In *LLCL* filters, L_{21} is mostly used to attenuate each harmonic around the twice of the switching frequency down to 0.3% and it can be articulated as in (12) , where $J_1(2\pi\alpha), J_3(2\pi\alpha)$, and $J_5(2\pi\alpha)$ are the integrals of the Bessel function corresponding to the sideband harmonics at the frequency of $(2\omega_s + \omega_0), (2\omega_s + 3\omega_0), and (2\omega_s + 5\omega_0)$.

$$J = max(|J_1(2\pi\alpha|), |J_3(2\pi\alpha|), |J_5(2\pi\alpha|) \tag{16}$$

$$\frac{(V_{dc}/\pi) \times J \times |G_{v_i \to i_g}(j2\omega s)|}{I_{ref}} \leq 0.3 \tag{17}$$

For a *L(LCL)*$_2$ filter, because of the additional L_fC_f resonate circuit, the current harmonics around the double of switching frequency satisfy the requirements of IEEE 519-2014 with far more ease. Therefor L_{21} is replaced by a portion of L_{11}.
5) The resonant frequency can be calculated by setting the dominator of equations (10) or (11) to zero, after replacing "s" with "jω". If it does not satisfy the requirement 3, absorbed reactive power can be changed and return to step 2. Or the tolerable current ripple can be adjusted again and return to step 1.
6) Quality factor of each resonant branch should be $10 \leq Q \leq 50$,which can be calculated as

$$Q = \frac{1}{R_f}\sqrt{\frac{L_f}{C_f}} \tag{18}$$

where R_f is the gaped equivalent resistance of the inductors in the resonant branches (L_{f1} and L_{f2}).

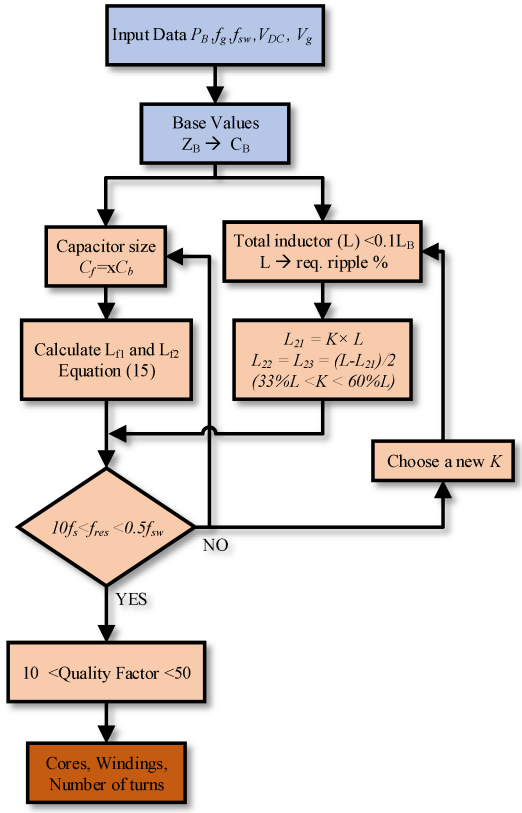

Fig. 6. Flowchart of the parameter design procedure of $L(LCL)_2$ filter.

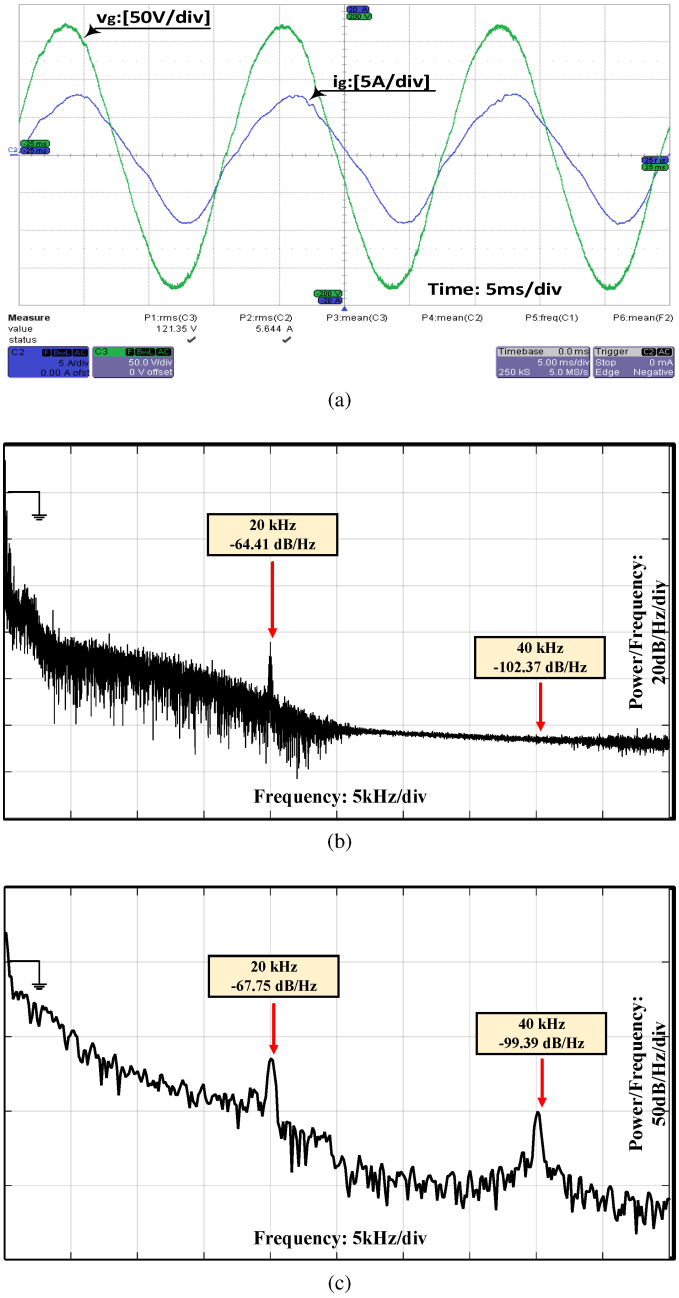

Fig. 7. *LLCL* filter. (a) Grid voltage and grid-side current waveforms. (b) Power density spectrum of grid-side current (Experimental setup). (c) Power density spectrum of grid-side current (Simulation)

The most important limitations such as the voltage drop across the inductor, the capacitive reactive power, and the amplitude of the harmonic currents should be considered, while the design process is iterative with the $L(LCL)_2$ parameter values adjusted. The algorithm for designing the $L(LCL)_2$ filter is shown in Fig. 6.

B. Design example

Once designing a high-order filter for power inverters, the base impedance of the system should be identified. So the base values of the total impedance, inductance, and capacitance are defined as (20)

$$Z_b = \frac{v_g}{P_{rated}}, L_b = \frac{Z_b}{\omega_b}, C_b = \frac{1}{\omega_b Z_b} \tag{19}$$

Where ω_b is the grid frequency and P_{rated} is the rated active power of the inverter. Considering the constrains addressed in section II−A, and under the condition of that f_s= 20 kHz, V_{dc} = 350V, P_{rated} = 700W, grid phase to ground voltage is 120 V/60 Hz, and the sine-triangle, and asymmetrical regular sampled PWM, then, the attenuation of the current harmonics focused in the design processes of the $L(LCL)_2$ filter can be derived as:

1) Adopting the 7.7% impedance for the inverter-side inductor, the inverter-side inductor is selected to be 4.2 mH. For an *LLCL* filter, L_{21} mainly depends on the objective to attenuate each harmonic around the switching frequency down to 0.3%, but for the $L(LCL)_2$ filter, owing to the $L_{f2}C_{f2}$ resonate circuit, the current harmonics around the twice of the switching frequency is approximately eliminated. Therefore, the calculated inductance for inverter side inductance of traditional *LLCL* filter is split into three smaller inductances. The first part has a value of L_{12}= 2.2 mH (about 53% of calculated inductance of *LLCL* filter) that can satisfy all requirements of grid side inverter, then L_{22}=1 mH and L_{32}=1 mH.
2) The total capacitance to achieve maximum reactive power absorbed at rated conditions (C_{f1} + C_{f2}) ≤ 0.05 C_b , the capacitor value is designed to C_{f1} + C_{f2} = 2 μF to limit the reactive power to 1.55%. If some of the

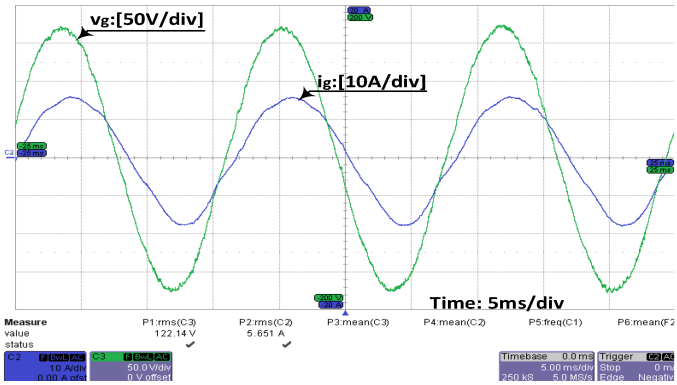

(a)

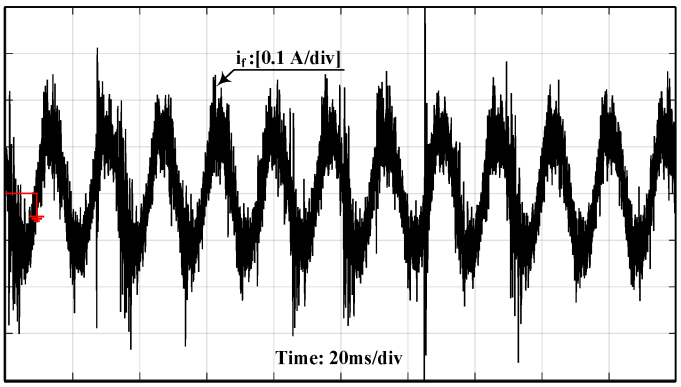

(a)

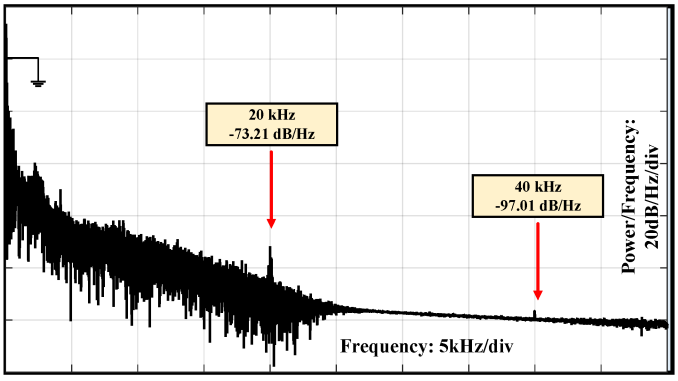

(b)

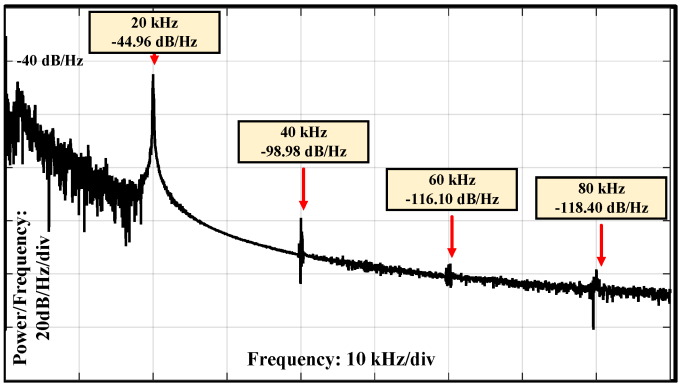

(b)

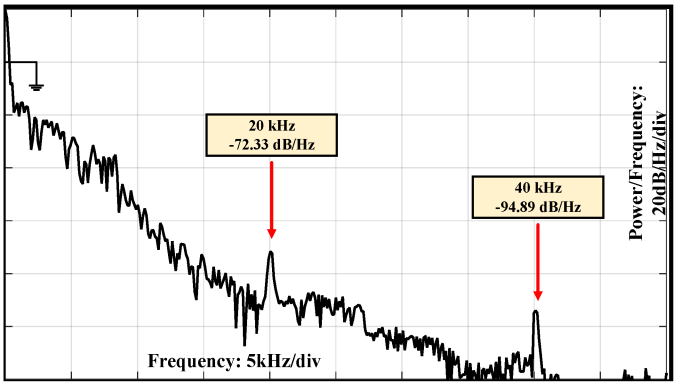

(c)

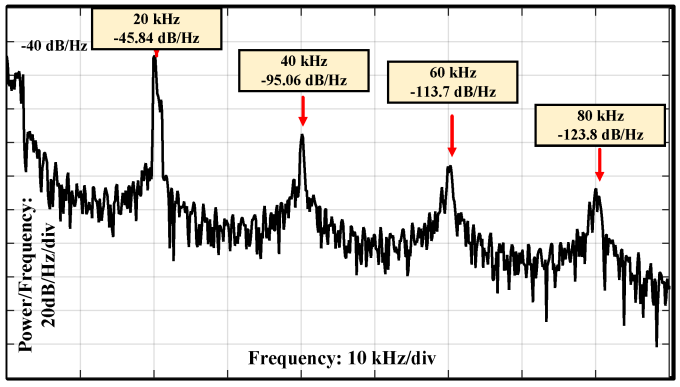

(c)

Fig. 8. $L(LCL)_2$ filter. (a) Grid voltage and grid-side current waveforms. (b) Power density spectrum of grid-side current (Experimental setup). (c) Power density spectrum of grid-side current (Simulation).

Fig. 9. (a) L_f-C_f current of *LLCL* filter . (b) Power spectral density of L_f-C_f current in *LLCL* filter (Experimental setup). (b) Power spectral density of L_f-C_f current in *LLCL* filter (Simulation).

constraints cannot be met, it should be increased to the limit of 5%.

3) The grid-side inductor of L_{21} is removed in the $L(LCL)_2$ filter, but L_{22} and L_{23} are two sections of the split filter and both of them has the value of 1mH.
4) The consequent resonance frequency is 3.88 kHz for the *LLCL* and the $L(LCL)_2$ filter has two resonant frequencies of 4.12 kHz and 8.01 kHz, which all are lower than one half of the switching frequency and bigger than one sixth of the switching frequency.
5) The quality factor of resonant branches is chosen to be 50, and the equivalent resistor value of R_{f1} is 0.16 and R_{f2} is 0.08 Ω.

IV. Simulation and Experimental Results

In order to confirm the effectiveness of the proposed $L(LCL)_2$ filter on suppressing the current harmonics, a 700-W prototype of the single-phase full-bridge grid-tied inverter with the "STM32F4" Microcontroller is constructed. In addition a Matlab Simulink-based study is carried out to assess the experimental analysis. The experimental parameters of the filter are the same as those for simulations listed in Table I.

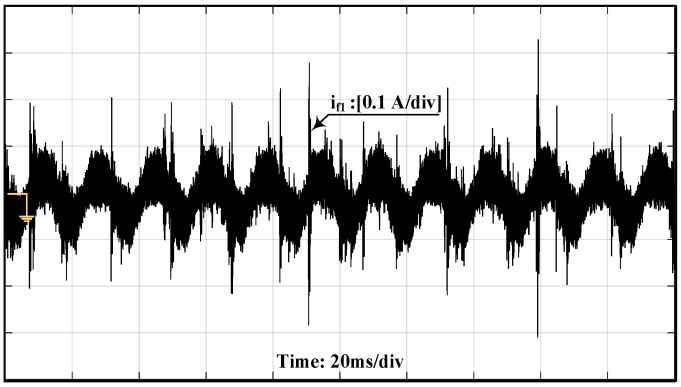

(a)

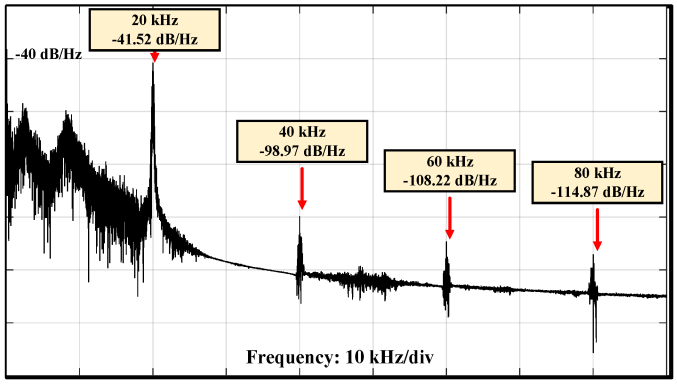

(b)

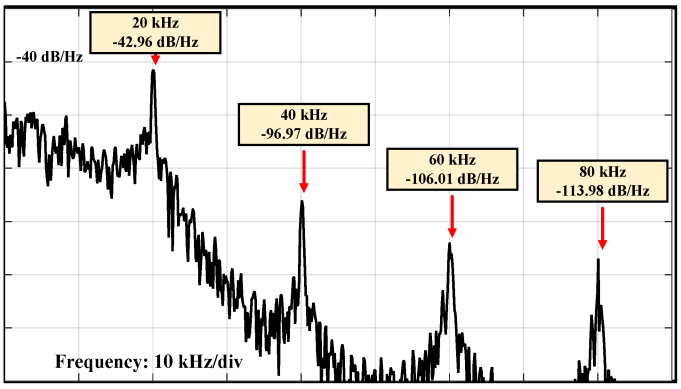

(c)

Fig. 10. (a) Current of switching frequency trap L_{f1}-C_{f1} of modified *LLCL* filter. (b) Power spectral density of L_{f1}-C_{f1} current in *L(LCL)*$_2$ filter (Experimental setup). (c) Power spectral density of L_{f1}-C_{f1} current in *L(LCL)*$_2$ filter (Simulation).

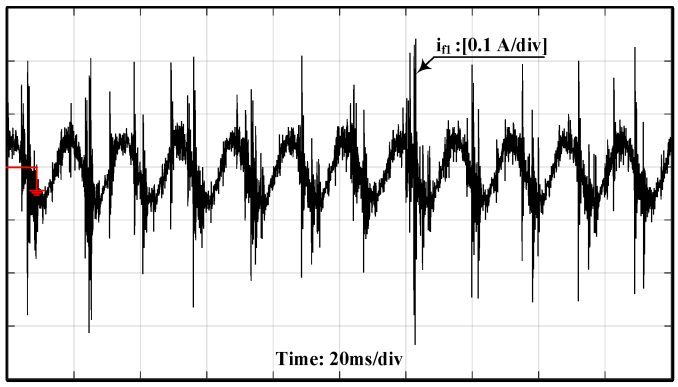

(a)

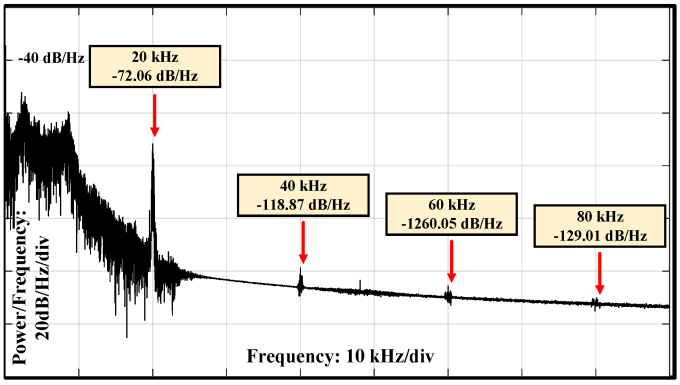

(b)

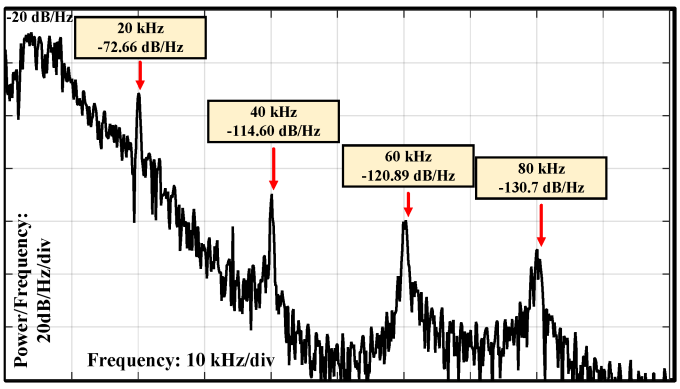

(c)

Fig. 11. (a) Current of double of switching frequency trap L_{f2}-C_{f2} of *L(LCL)*$_2$ filter . (b) Power spectral density of L_{f2}-C_{f2} current in *L(LCL)*$_2$ filter (Experimental setup). (c) Power spectral density of L_{f2}-C_{f2} current in *L(LCL)*$_2$ filter (Simulation).

The experiments are evaluated and investigated under the given conditions of f_s = 20 kHz, V_{dc} = 350 V, v_g = 120 V/60 Hz, P_{rated} = 700 W, and SPWM strategy is used in the inverter and the DC link voltage is kept at 350 V.

Case I is the traditional *LLCL* filter strategy and Case II is the *L(LCL)*$_2$ filter strategy with an extra trap at 40 kHz. Figs. 7-11 show important system measurements that are captured by a LaCory WaveRunner 64Xi oscilloscope in experimental tests.

Figs. 7 and 8 show the grid side current-voltage waveforms and the power density spectrum of the grid-side current for cases I and II respectively. Figs. 7(b) and Fig. 8(b) illustrate that the amplitude of the dominant harmonic current at 20 kHz is reduced by 8.80 dB/HZ from case I to case II, but at 40 kHz it increased from -102.37 dB/Hz (case I) to -97.01 dB/Hz (case II). So the most dominant current harmonics are diminished even more than previous design. However a small increase occurred at double of switching frequency but as the power density is too small (-97.01 dB/Hz), it can be neglected. Therefore, the size of the filter is reduced, and as a result the the total loss is decreased. In addition the performance of the filter is improved. Figs. 7 (c) and 8 (c) show the simulation

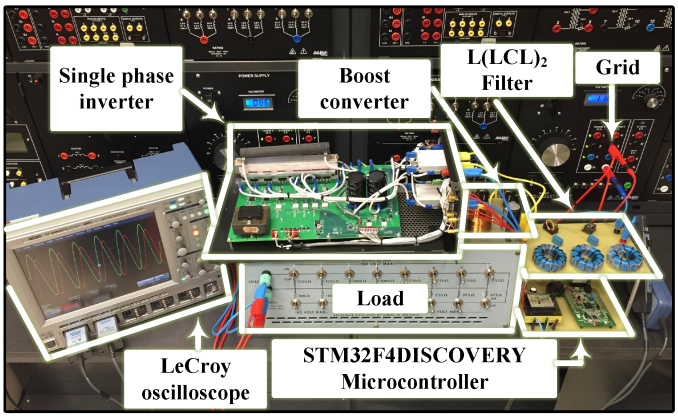

Fig. 12. Experimental Setup

TABLE I
PARAMETERS USED FOR SIMULATIONS

Elements	Parameters	Values
Inverter	DC link voltage (V_{dc})	350 V
	Switching frequency (f_s)	20 kHz
	Rated power (P_{rate})	700 w
AC Grid	Grid phase voltage (V_g)	120 V
	Grid frequency (f_0)	60 Hz
Modified LLCL filter	Converter side inductor (L_1)	2.2mH
	Grid side inductors ($L_{21} = L_{22}$)	1 mH
	Resonant circuit inductor (L_{f1})	63.3 μH
	Resonant circuit inductor (L_{f2})	15.83 μH
	Resonant circuit capacitors ($C_{f1} = C_{f2}$)	1 μF
	Equivalent resistance of the inductor (R_{f1})	0.16 Ω
	Equivalent resistance of the inductor (R_{f2})	0.08 Ω
LLCL filter	Converter side inductor (L_1)	4.2 mH
	Grid side inductor (L_2)	1.2 mH
	Resonant circuit inductor (L_f)	31.67 μH
	Resonant circuit capacitor (C_f)	2 μF
	Equivalent resistance of the inductor (R_f)	0.11 Ω

results of power density spectrum of grid-side current. As it can be seen the experimental results are in accordance to the simulation graphs.

The currents flowing through the resonant branches for Case I and Case II are shown in Figs. 9 to 11 while the grid current is 5.8 A and the voltage is 120 V. The magnitude of the currents in $L_{f1}C_{f1}$ and $L_{f2}C_{f2}$ traps are almost half of L_fC_f trap and that is because the impedance of the both traps of *L(LCL)*$_2$ filter is 2.652 kΩ (at 60 Hz) but the *LLCL* filter has an impedance of 1.326 kΩ. Also, it can be seen that the power density of current harmonics at the switching frequency and multiples of the switching frequency are almost the same in L_fC_f branch of *LLCL* and $L_{f1}C_{f1}$ branch of the *L(LCL)*$_2$ filter. In addition to that more attenuation occurs at $L_{f2}C_{f2}$. Then in Figs. 9 (c) - 11 (c) simulation results are depicted which are quite close to the hardware experimental results.

The measured total harmonic distortion (THD)% of i_g in Cases I, and II are 3.72% and 2.94% which shows the effectiveness of the designed filter in improving the THD of the grid current.

The photo of the *L(LCL)*$_2$-filter-based inverter system is shown in Fig. 12. For building the inductances of *LLCL* and *L(LCL)*$_2$ filters Ferrite cores with N87 material and epoxy coating is used.

A. Analysis and Discussion

From the simulation and experimental results, the following can be seen.

1) In both Cases, the dominating harmonic current meets the recommendation of IEEE 519-2014 in the experiment, however the 20kHz current harmonic reduced and the 40kHz current harmonic has the same value.
2) The value of the grid-side inductor in reduced in cases II, so the voltage drop during operation and thereby the dc link voltage are the same.
3) The value of the total inductor of *L(LCL)*$_2$ filter is reduced by a factor of 22.22%, compared to that of the *LLCL* filter.
4) The reactive power in the newly designed filter is the same as traditional *LLCL* filter C_{f1}+C_{f2}=C_f.
5) In general, the experimental results are in acceptable agreement with the theoretical study, particularly with regard to the harmonic current attenuation around the switching frequency and the double of the switching frequency.

V. CONCLUSION

In this paper, the principle of the conventional *LLCL* filter and parameter design of the *L(LCL)*$_2$ filters has been proposed. Since grid side inductance (L_{21}) of the *LLCL* filter is mainly decided by the harmonic currents around the double of the switching frequency instead of those around the switching frequency, it has been replaced by a small trap at double of switching frequency. Compared to the *LLCL* filter, this replacement results in reduction of the total inductance size and hence total loss of the filter. The inverter side inductance is divided into three parts to place resonant branches in between them. Therefore, the *L(LCL)*$_2$ filter has less copper loss and better performance at high order harmonics attenuation. In the proposed design, the maximum power factor variation remained unchanged and the THD has improved by 18.61%.

A 700 W single-phase grid-tied inverter is designed to compare the characteristics of the conventional *LLCL* filter and the suggested *L(LCL)*$_2$ filter through experimental results. The results validate the value of the inductors of the *L(LCL)*$_2$ filter, which is reduced by a factor of 22.22%, compared to that of the *LLCL* filter, when the modulation index is 0.9

REFERENCES

[1] A. Anzalchi and A. Sarwat, "Analysis of carbon tax as an incentive toward building sustainable grid with renewable energy utilization," in *Green Technologies Conference (GreenTech), 2015 Seventh Annual IEEE*, April 2015, pp. 103–109.
[2] A. Anzalchhi and A. Sarwat, "Artificial neural network based duty cycle estimation for maximum power point tracking in photovoltaic systems," in *SoutheastCon 2015*, April 2015, pp. 1–5.
[3] M. Lindgren and J. Svensson, "Connecting fast switching voltage source converters to the grid-harmonic distortion and its reduction," in *Stockholm Power Tech. Conf.*, June 18-22 1995, pp. 191–195.
[4] M. Liserre, F. Blaabjerg, and S. Hansen, "Design and control of an lcl-filter-based three-phase active rectifier," *Industry Applications, IEEE Transactions on*, vol. 41, no. 5, pp. 1281–1291, Sept 2005.

978-1-4673-8672-2/15/$31.00 © 2016 IEEE

[5] I. Gabe, V. Montagner, and H. Pinheiro, "Design and implementation of a robust current controller for vsi connected to the grid through an lcl filter," *Power Electronics, IEEE Transactions on*, vol. 24, no. 6, pp. 1444–1452, June 2009.

[6] H.-G. Jeong, K.-B. Lee, S. Choi, and W. Choi, "Performance improvement of lcl-filter-based grid-connected inverters using pqr power transformation," *Power Electronics, IEEE Transactions on*, vol. 25, no. 5, pp. 1320–1330, May 2010.

[7] J. Dannehl, F. Fuchs, and P. Thogersen, "Pi state space current control of grid-connected pwm converters with lcl filters," *Power Electronics, IEEE Transactions on*, vol. 25, no. 9, pp. 2320–2330, Sept 2010.

[8] P. Channegowda and V. John, "Filter optimization for grid interactive voltage source inverters," *Industrial Electronics, IEEE Transactions on*, vol. 57, no. 12, pp. 4106–4114, Dec 2010.

[9] Y. Jiao, S. Lu, and F. Lee, "Switching performance optimization of a high power high frequency three-level active neutral point clamped phase leg," *Power Electronics, IEEE Transactions on*, vol. 29, no. 7, pp. 3255–3266, July 2014.

[10] M. Huang, F. Blaabjerg, Y. Yang, and W. Wu, "Step by step design of a high order power filter for three-phase three-wire grid-connected inverter in renewable energy system," in *Power Electronics for Distributed Generation Systems (PEDG), 2013 4th IEEE International Symposium on*, July 2013, pp. 1–8.

[11] W. Wu, Y. Sun, Z. Lin, Y. He, M. Huang, F. Blaabjerg, and H.-H. Chung, "A modified llcl filter with the reduced conducted emi noise," *Power Electronics, IEEE Transactions on*, vol. 29, no. 7, pp. 3393–3402, July 2014.

[12] W. Wu, Y. Sun, M. Huang, X. Wang, H. Wang, F. Blaabjerg, M. Liserre, and H.-H. Chung, "A robust passive damping method for llcl-filter-based grid-tied inverters to minimize the effect of grid harmonic voltages," *Power Electronics, IEEE Transactions on*, vol. 29, no. 7, pp. 3279–3289, July 2014.

[13] W. Wu, Y. Sun, Z. Lin, T. Tang, F. Blaabjerg, and H.-H. Chung, "A new lcl -filter with in-series parallel resonant circuit for single-phase grid-tied inverter," *Industrial Electronics, IEEE Transactions on*, vol. 61, no. 9, pp. 4640–4644, Sept 2014.

[14] D. Pan, X. Ruan, C. Bao, W. Li, and X. Wang, "Capacitor-current-feedback active damping with reduced computation delay for improving robustness of lcl-type grid-connected inverter," *Power Electronics, IEEE Transactions on*, vol. 29, no. 7, pp. 3414–3427, July 2014.

[15] D.Pan, X.Ruan, C.Bao, W.Li, and X.Wang, "Magnetic integration of the lcl filter in grid-connected inverters," *Power Electronics, IEEE Transactions on*, vol. 29, no. 4, pp. 1573–1578, April 2014.

[16] W. Wu, Y. He, and F. Blaabjerg, "An llcl power filter for single-phase grid-tied inverter," *Power Electronics, IEEE Transactions on*, vol. 27, no. 2, pp. 782–789, Feb 2012.

[17] D. Holmes and T. Lipo, *Modulation of SinglePhase Voltage Source Inverters*. Wiley-IEEE Press, 2003, pp. 155–213. [Online]. Available: http://ieeexplore.ieee.org/xpl/articleDetails.jsp?arnumber=5311953

[18] "Ieee recommended practice and requirements for harmonic control in electric power systems," *IEEE Std 519-2014 (Revision of IEEE Std 519-1992)*, pp. 1–29, June 2014.

[19] "Ieee application guide for ieee std 1547(tm), ieee standard for interconnecting distributed resources with electric power systems," *IEEE Std 1547.2-2008*, pp. 1–217, April 2009.

[20] Y. Lang, D. Xu, S. Hadianamrei, and H. Ma, "A novel design method of lcl type utility interface for three-phase voltage source rectifier," in *Power Electronics Specialists Conference, 2005. PESC '05. IEEE 36th*, June 2005, pp. 313–317.

[21] B. Bolsens, K. De Brabandere, J. Van den Keybus, J. Driesen, and R. Belmans, "Model-based generation of low distortion currents in grid-coupled pwm-inverters using an lcl output filter," *Power Electronics, IEEE Transactions on*, vol. 21, no. 4, pp. 1032–1040, July 2006.

[22] M. Liserre, F. Blaabjerg, and S. Hansen, "Design and control of an lcl-filter based three-phase active rectifier," in *Industry Applications Conference, 2001. Thirty-Sixth IAS Annual Meeting. Conference Record of the 2001 IEEE*, vol. 1, Sept 2001, pp. 299–307 vol.1.

[23] M. Huang, F. Blaabjerg, P. C. Loh, and W. Wu, "Stability analysis and active damping for llcl-filter based grid-connected inverters," in *Power Electronics Conference (IPEC-Hiroshima 2014 - ECCE-ASIA), 2014 International*, May 2014, pp. 2610–2617.

978-1-4673-8672-2/15/$31.00 © 2016 IEEE